# Rupture directions of hydraulic fractures derived from microseismic waveform complexity

*Qiankun Zuo[1*], Youcai Tang[1], Fenglin Niu[1, 2], Xiaobo Meng[1], Deyou Xu[1], Ziliang Wang[1]*
*1 State Key Laboratory of Petroleum Resource and Prospecting, and Unconventional Natural Gas Institute, China University of Petroleum, Beijing 102249,China*
*2 Departments of Earth Science, MS-126, Rice University, Houston, Texas 77005, USA*

## Summary

The waveforms of microseismic events during hydraulic fracturing are complicated sometimes and could not be interpreted as simple point sources. If we assume that the waveforms are a superimposition of several subevents occurred on the same fracture plane with different initial times, then we can determine the stepover rupture direction by identifying and locating these subevents. Real data analysis show that stepover rupture directions derived from waveform complexity are consistent with temporal-spatial distribution of microseismic events. The results could also be indicators of pumping fluid flow directions during and after hydraulic performance.

## Introduction

Hydraulic fracturing is an effective method to stimulate tight reservoirs. It involves pumping high-pressure fluid into reservoir rocks to force the opening of cracks, which could allow oil and gas to flow freely. Microseismic monitoring is an effective method to evaluate the hydraulic performance and to avoid undesirable ruptures. The temporal-spatial distribution and source mechanisms of microseismic events are usually used to monitor the opening of cracks associated with fluid injection and to evaluate stimulated rock volume. Downhole monitoring has advantage of high quality seismic data, and had been applied in many hydraulic fracturing experiments (Jones et al. 2014; Zhou et al. 2016). More and more new techniques have been developed to exact more information from microseismic data, such as template search (Meng et al., 2016) based on waveform similarity, double difference tomography (Chen et al., 2016) based on relative arrival time information However, these methods treat the microseismic events as point sources and ignore the complexity of events source which could shed light on rupture directions and so on.

The waveforms of microseismic events are complicated sometimes and could not be interpreted as simple point sources. Figure1 shows examples for simple waveform and complicated waveform of microseismic events from a downhole monitoring. The simple waveform in Figure 1a is a typical microseismic event and could be interpreted as a point source. However, the waveforms in Figure 1b seem to be a superimposition of several subevents with different arrival times. The waveforms of P wave and S wave have similar characteristics that could indicate a complex source.

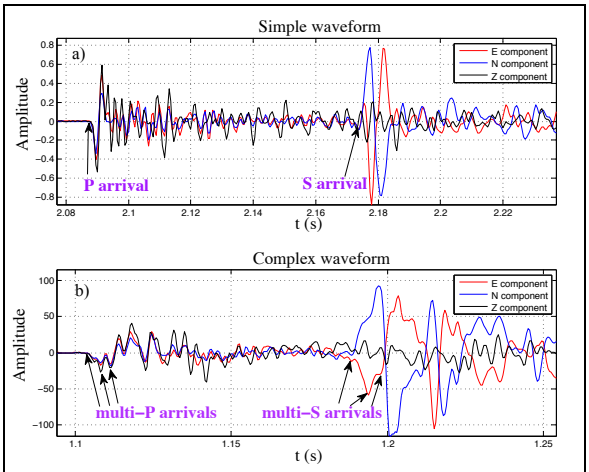


Figure1: Examples of waveform recorded during hydraulic fracturing. a) Simple waveform of microseismic event; b) complex waveform of microseismic events.

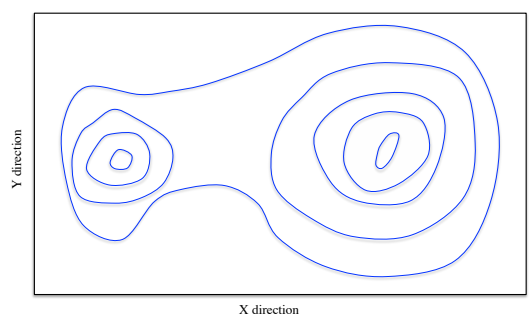


Figure2: Slip distribution of several subregions of one fault plane.

If the rupture process on a fracture plane is simple, the direct P and S waves will be like pulses. However, the fracture plane is complicated in many cases. For example, if barriers exist in the plane, then stepover rupture will occur and the slip distribution will split into several subregions (Figure 2). Consequently, the wave train of P and S wave will become complicated and seem as a

superimposition of several subevents with different arrival times.

The stepover rupture bring troubles in microseismic events arrival picks and locations. However, the relative slip distribution of these subregion could help us to determine the rupture propagate directions and subsequently the direction of fracture plane.

In this study, we focus on the stepover rupture/multi-subevent to determine the rupture direction.

## Method

The main purpose of this study is to determine rupture directions in fracture planes from microseismic waveform complexities. The method can be split into two parts:

(1) Subevent identification
The waveforms are superimpositions of several subevents with different arrival times. The waveforms of subevents interfere with each other and are difficult to isolate them completely. However, the maximum waveforms of the subevents separate from each other (Figure 3).

If we assume that the maximum waveforms of subevents associate with the maximum slip of each subrupture (Figure 2), we can locate the maximum slip by using the maximum waveforms. We used half period of waveforms around the maximum waveforms to locate subevents.

Assuming in homogeneous and isotropic-layered media, microseismic events must be constrained by azimuthal information along with P and S wave arrivals when using downhole arrays (De Meersman et al. 2006). We defined the object function as:

$$\Phi = \sum_{i=1}^{N}\left[w_1\left(t_{pi} - TP_i - T_0\right)^2 + w_2\left(t_{si} - TS_i - T_0\right)^2 + w_3\left(Az^{obs}{}_i - Az^{cal}{}_i\right)^2\right]$$

Where, N is the station number, tpi and tsi is the observed arrival of maximum waveform for P and S waves, respectively. $T_0$ is the origin time. w1, w2 and w3 are weighting factor. Az is the raypath azimuth determined by using P wave particle motion (Figure 3). It is obtained from covariance method which has been applied widely downhole monitoring (Caffagni et al. 2016). By minimizing equation (3), we can obtain source location.

(2) Rupture direction determination
Once all subevents have been located, we can determine rupture directions or the fracture plane directions.

Assuming that in a fracture plane, the stepover rupture propagates from earlier subevents to later subevents, we can determine the rupture direction by using a vector pointing from earlier subevents to later subevents.
If only two subevents could be identified and located, we can only determine the strike of the rupture propagate direction. If three or more subevents could be identified and located, the stepover rupture direction along with the geometry of the fracture plane can be determined in 3D space.

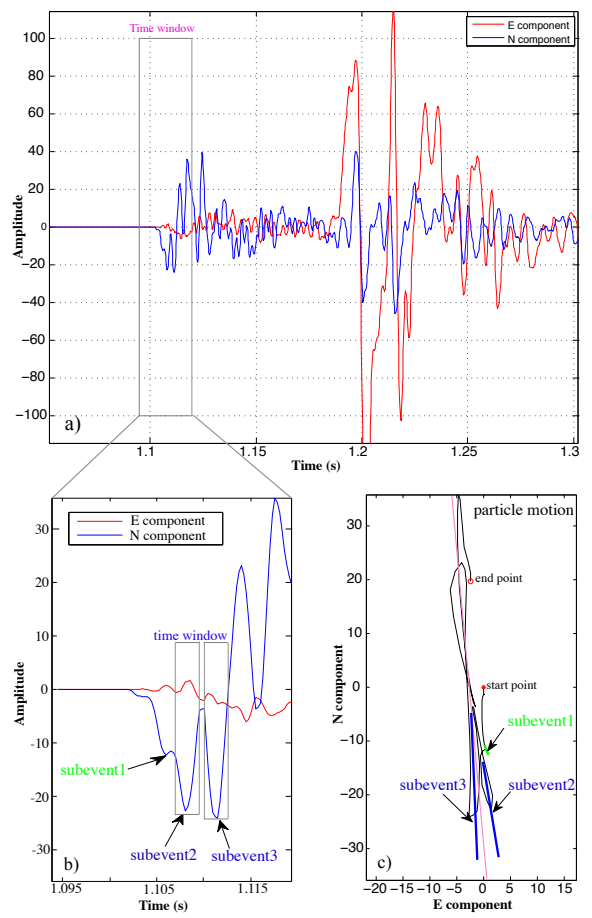


Figure 3: Polarization analysis of one event and its phase's arrivals. a) EN component waveform; b) zoom in of a); c) hodogram corresponding three sub events in b);

## Real data

We deployed a downhole array with 20-level three-component geophones in a deviated well to study the dynamic processes involved in hydraulic fracturing in

Sichuan Basin, China (Figure 4). Geophones ranged from 2120m to 2405m depths with a 15-m interval. The downhole seismic array detected a total of 386 microseismic events with high signal-to-noise ratios (SNRs) during the last stage (marked by blue rectangular in Figure 4). The velocity model used in events location was determined from well log data and was calibrated by the perforation data of the last stage.

During the last stage, we selected 9 events with clear stepover rupture. Figure 4 shows the waveforms of one event with three subevents. P and S first arrival are marked by IPU0 and ISU0, subevent1 is very weak, and subevent2 and subevent3 are marked by tp1, tp2 for P arrivals and ts1, ts2 for S arrivals.

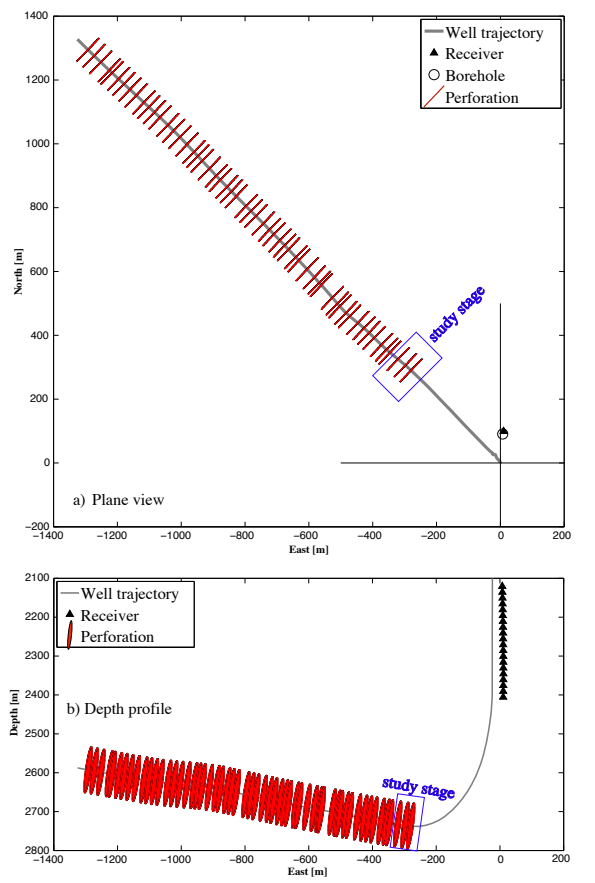


Figure 4: Plane view (a) and profile view (b), blue rectangular area is our study area of stage19.

## Results

Figure 5 shows the results of the rupture direction determined from waveform complexity. The red circles denote the event locations derived from first arrivals for P and S wave. These locations are usually interpreted as the initial of ruptures. Blue and green dots denote the locations for subevents determined from the maximum waveforms in each event. The subevents shown as blue dots occurred earlier than the subevents shown as green dots.

Each group of red circle, blue dot and red dot could determine a fracture plane. We draw blue lines between associated subevents and black lines to their corresponding rupture initials (red circles).

The arrows pointing to the last subevents (green dots) represent the rupture directions. These directions are consistent with the temporal-spatial distribution of microseismic events.

(1) The strikes of the fracture planes are consistent with the trend of the spatial distribution of microseismic events.

(2) During the hydraulic performance, microseismic events migrated outward from the perforation points along with pumping fluid flow forward. Our stepover ruptures also propagate in the same directions.

After the pumping stopped, microseismic events migrated backward to the well along with fluid drew back. During this stage, the stepover ruptures also show a similar behavior.

## Conclusion

We derived rupture directions of hydraulic fractures from microseismic waveform complexity. Subevents could be identified and located by using their maximum waveforms. Real data analysis show that stepover rupture directions derived from waveform complexity are consistent with temporal-spatial distribution of microseismic events. The results could also be indicators of fluid flow directions.

## Acknowledgement

We thank the Sichuan Geophysical Company of CNPC Chuanqing Drilling Engineering Company Limited for providing the monitoring data. This research is supported by the National Program on key Basic Research Project (973 Program, grant number SQ2015CB021174, and Science Foundation of China University of Petroleum，Beijing, NO. 2462013YJRC014).

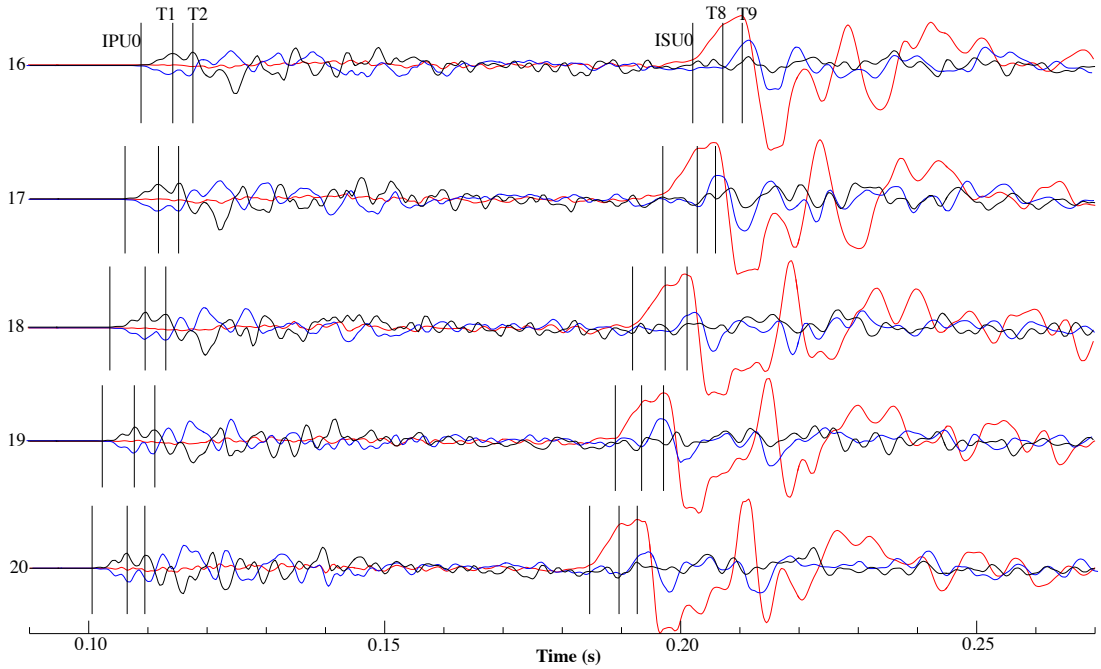


Figure5: Phases picks of five station of one event (Note: red, blue and black are E, N and Z component, respectively).

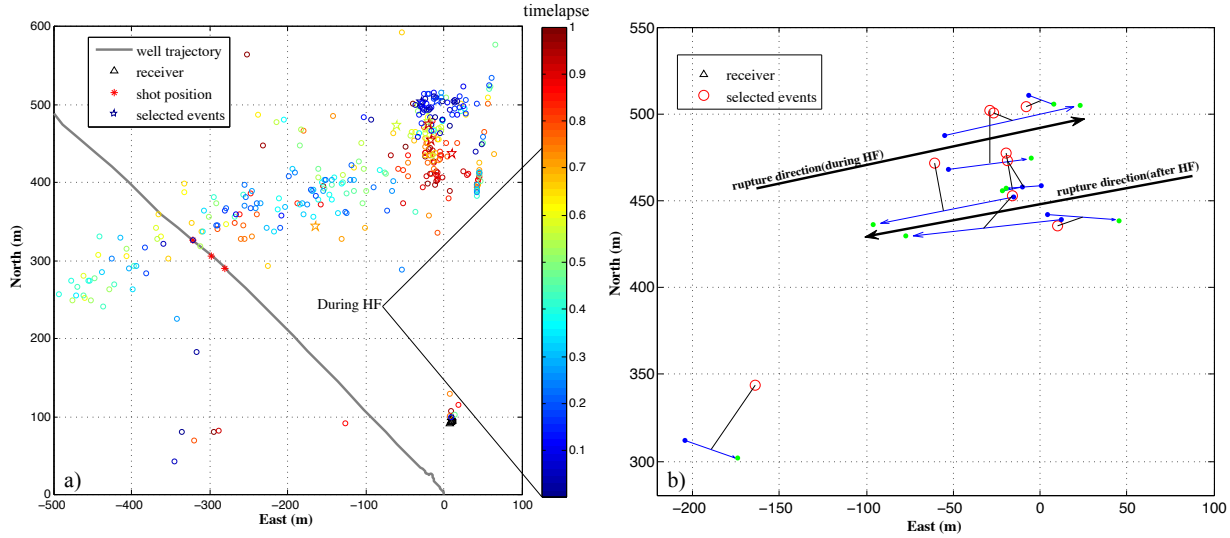


Figure6: a) Microseismic events location in plan view, color circles represent different time lapse; b) analysis selected events (red circles) in a) to get rupture direction which is indicated by blue arrows.

**EDITED REFERENCES**

Note: This reference list is a copyedited version of the reference list submitted by the author. Reference lists for the 2017 SEG Technical Program Expanded Abstracts have been copyedited so that references provided with the online metadata for each paper will achieve a high degree of linking to cited sources that appear on the Web.

**REFERENCES**

Caffagni, E., D. W. Eaton, J. P. Jones, and M. V. D. Baan, 2016, Detection and analysis of microseismic events using a Matched Filtering Algorithm (MFA): Geophysical Journal International, **206**, 644–658, https://doi.org/10.1093/gji/ggw168.

Chen, Y. K., H. J. Zhang, Y. Miao, Y. Zhang, and Q. Liu, 2017, Back azimuth constrained double-difference seismic location and tomography for downhole microseismic monitoring: Physics of the Earth and Planetary Interiors, **264**, 35–46, https://doi.org/10.1016/j.pepi.2016.10.003.

Chen, Z., B. Cox, and C. Perkins, 2013, The influence of HTI anisotropy on microseismic event location–a case study from a tight gas field in British Columbia: 83th SEG Annual International Meeting, Expanded Abstracts, 2003–2007, https://doi.org/10.1190/segam2013-0034.1.

De Meersman, K., M. Van der Baan, and J. M. Kendall, 2006, Signal extraction and automated polarization analysis of multicomponent array data: Bulletin of the Seismological Society of America, **96**, 2415–2430, https://doi.org/10.1785/0120050235.

Eisner, L., B. J. Hulsey, P. Duncan, D. Jurick, W. Heigl, and W. Keller, 2010, Comparison of surface and borehole locations of induced seismicity: Geophysical Prospecting, **9**, 809–820, https://doi.org/10.1111/j.1365-2478.2010.00867.x.

Jones, G. A., J. M. Kendall, I. D. Bastow, and D. G. Raymer, 2014, Locating microseismic events using borehole data: Geophysical Prospecting, **62**, 34–49, https://doi.org/10.1111/1365-2478.12076.

Meng, X. B., H. C. Chen, F. L. Niu, Y. C. Tang, and Q. K. Zuo, 2016, Detection and location for microseismic events recorded by single-downhole acquisition with crosscorrelation method: 86th SEG Annual International Meeting, Expanded Abstracts, 2745–2749, https://doi.org/10.1190/segam2016-13947703.1.

Zhou, H., W. Zhang, and J. Zhang, 2016, Downhole microseismic monitoring for low signal-to-noise ratio events: Journal of Geophysics and Engineering, **13**, 805–816, https://doi.org/10.1088/1742-2132/13/5/805.